

1 **Title:** Susceptible host availability modulates climate effects on dengue dynamics

2 **Authors:** Nicole Nova<sup>1\*</sup>, Ethan R. Deyle<sup>2,3</sup>, Marta S. Shocket<sup>1,4</sup>,

3 Andrew J. MacDonald<sup>1,5</sup>, Marissa L. Childs<sup>6</sup>, Martin Rypdal<sup>7</sup>,

4 George Sugihara<sup>2</sup>, and Erin A. Mordecai<sup>1</sup>

5 **Affiliations:** <sup>1</sup>Department of Biology, Stanford University, Stanford, CA, USA.

6 <sup>2</sup>Scripps Institution of Oceanography, University of California San

7 Diego, La Jolla, CA, USA.

8 <sup>3</sup>Department of Biology, Boston University, Boston, MA, USA.

9 <sup>4</sup>Department of Ecology and Evolutionary Biology, University of

10 California, Los Angeles, CA, USA.

11 <sup>5</sup>Earth Research Institute & Bren School of Environmental Science and

12 Management, University of California Santa Barbara, Santa Barbara,

13 CA, USA.

14 <sup>6</sup>Emmett Interdisciplinary Program in Environment and Resources,

15 Stanford University, Stanford, CA, USA.

16 <sup>7</sup>Department of Mathematics and Statistics, UiT The Arctic University

17 of Norway, Tromsø, Norway.

18 **\*Correspondence email:** [nicole.nova@stanford.edu](mailto:nicole.nova@stanford.edu)

19 **Keywords:** Arbovirus, climate, dengue, empirical dynamic modeling, forecasting,

20 vector-borne disease, rainfall, susceptible population size, temperature

## 21 **Abstract**

22 Experiments and models suggest that climate affects mosquito-borne disease  
23 transmission. However, disease transmission involves complex nonlinear  
24 interactions between climate and population dynamics, which makes detecting  
25 climate drivers at the population level challenging. By analyzing incidence data,  
26 estimated susceptible population size, and climate data with methods based on  
27 nonlinear time series analysis (collectively referred to as empirical dynamic  
28 modeling), we identified drivers and their interactive effects on dengue dynamics in  
29 San Juan, Puerto Rico. Climatic forcing arose only when susceptible availability was  
30 high: temperature and rainfall had net positive and negative effects, respectively. By  
31 capturing mechanistic, nonlinear, and context-dependent effects of population  
32 susceptibility, temperature, and rainfall on dengue transmission empirically, our  
33 model improves forecast skill over recent, state-of-the-art models for dengue  
34 incidence. Together, these results provide empirical evidence that the  
35 interdependence of host population susceptibility and climate drive dengue  
36 dynamics in a nonlinear and complex, yet predictable way.

## 37 INTRODUCTION

38 Ecological systems are complex, nonlinear, and dynamic. Understanding their  
39 mechanistic drivers is increasingly important in a rapidly changing world. Because  
40 of this complexity, mechanistic studies are often conducted in simplified, controlled  
41 environments at small scales. Connecting these experimental results with larger-  
42 scale emerging patterns remains a challenge but is nonetheless imperative for  
43 understanding the impacts of ecological change.

44 In concert with globalization and climate change, mosquito-borne diseases,  
45 and dengue in particular, are (re)emerging globally and spreading to higher  
46 latitudes (Kilpatrick & Randolph 2012; Ryan *et al.* 2019). Dengue virus—vectored  
47 primarily by urban *Aedes aegypti* (Kraemer *et al.* 2015)—places half of the global  
48 human population in 128 countries at risk of infection (Brady *et al.* 2012; Kraemer  
49 *et al.* 2019). In the absence of effective vaccines or treatments (Katzelnick *et al.*  
50 2017a; Sridhar *et al.* 2018), public health agencies rely on vector control to reduce  
51 dengue transmission (Erlanger *et al.* 2008). Effective vector control interventions  
52 require understanding the mechanisms linking climate, vector ecology, disease  
53 transmission, and host population susceptibility to better predict disease  
54 outbreaks—a major challenge.

55 Since *Aedes* spp. mosquitoes are sensitive to climate, including temperature  
56 and rainfall (Stewart Ibarra *et al.* 2013; Mordecai *et al.* 2019), we expect  
57 temperature and rainfall to be important drivers of dengue outbreaks. Although

58 temperature affects mosquito and viral traits in laboratory experiments (Watts *et al.*  
59 1987; Lambrechts *et al.* 2011; Mordecai *et al.* 2017), the relationship between  
60 temperature and dengue incidence in the field has been ambiguous (Caldwell *et al.*  
61 2020). Thus, temperature-dependent models have had mixed success predicting the  
62 timing and magnitudes of epidemics (Hii *et al.* 2012; Johansson *et al.* 2016; Johnson  
63 *et al.* 2018). Similarly, the rainfall–dengue relationship is complex, because the  
64 effect of rainfall on mosquitoes depends on local breeding habitat and human  
65 behavior. In some settings, rainfall fills container-breeding habitats for mosquitoes,  
66 increasing mosquito abundance and dengue incidence (Stewart Ibarra *et al.* 2013).  
67 By contrast, low rainfall can also facilitate dengue transmission by promoting water  
68 storage that serves as standing-water habitat for mosquitoes (Oliveira-lima *et al.*  
69 2000). Further, heavy rainfall can reduce mosquito abundance by flushing out  
70 larvae (Koenraadt & Harrington 2008). The net effect of climate on dengue  
71 therefore depends on many different mechanisms and is highly context-dependent.

72         Disease incidence also depends nonlinearly on susceptible availability,  
73 because epidemic growth slows as the population of susceptible individuals is  
74 exhausted (Anderson & May 1979; Dushoff *et al.* 2004; Mina *et al.* 2015; Pitzer *et al.*  
75 2015; Rypdal & Sugihara 2019). Further, susceptible availability may influence the  
76 effects of climate on dengue dynamics. However, such interactive effects are difficult  
77 to detect since susceptibility is difficult to observe, especially in endemic settings  
78 where multiple serotypes circulate and create a complex landscape of time-  
79 dependent and serotype-dependent immunity (Katzelnick *et al.* 2017b). Specifically,  
80 four serotypes of dengue regularly circulate in many regions: each provides long-

81 term serotype-specific (homologous) immunity and short-term (heterologous)  
82 cross-protection against other serotypes (dos Santos *et al.* 2017; Jiménez-Silva *et al.*  
83 2018; Hamel *et al.* 2019). Following a brief period of cross-protection, antibodies at  
84 a mid-range of titers can cause antibody-dependent enhancement of disease  
85 following heterologous, secondary infection, until titers decay to the point of nearly  
86 full heterologous susceptibility (Katzelnick *et al.* 2017b). Given this complex and  
87 dynamic immune landscape, directly detecting population susceptibility to  
88 circulating dengue virus at any point in time is difficult without longitudinal  
89 serology studies, which are not widely available (Gordon *et al.* 2013; Katzelnick *et*  
90 *al.* 2017b).

91 Previous prediction models of dengue outbreaks used phenomenological  
92 (Johansson *et al.* 2009b; Hii *et al.* 2012; Johnson *et al.* 2018) and mechanistic  
93 equation-based approaches (Tran *et al.* 2013; Liu-Helmersson *et al.* 2014; Morin *et*  
94 *al.* 2015; Mordecai *et al.* 2017), which may not fully capture interdependence  
95 between climate and susceptible availability. Phenomenological models may  
96 underperform when extrapolating past observed contexts, and equation-based  
97 mechanistic models rely on parameter estimates from laboratory studies  
98 engineered to isolate single mechanisms producing separate relationships between  
99 drivers and outcome, eliminating the complex interdependence at the population  
100 level. While laboratory studies provide robust validation of mechanisms  
101 (Lambrechts *et al.* 2011), the fixed relationships obtained from them do not  
102 necessarily translate into robust causal understanding for the complexity of field  
103 systems (Sugihara *et al.* 2012). Even if causality exists between two variables in such

104 a system, their correlation can switch signs during different time periods, resulting  
105 in a net correlation of zero (Deyle *et al.* 2016b). This temporal variation in the  
106 direction of correlation results from the nonlinear, state-dependent relationship  
107 between the variables (i.e., the effect depends on another variable's state).  
108 Conversely, even if two variables are consistently correlated, the association could  
109 be spurious due to a confounder.

110 To overcome these challenges, we used empirical dynamic modeling (EDM)  
111 (Sugihara *et al.* 2012)—a mechanistic, equation-free, data-driven approach that  
112 accounts for the context-dependence of ecological drivers to identify and model  
113 mechanisms driving dengue epidemics. EDM is based on reconstructing the  
114 essential system dynamics evident in time series, without assuming fixed  
115 relationships. This means relationships among variables can change through time to  
116 reflect that interactions among variables depend on context and system state. EDM  
117 does not require assumptions about the functional form of the model, but instead  
118 derives dynamic relationships empirically by constructing an attractor—a  
119 geometric object (i.e., curve or manifold) that embodies the rules for how  
120 relationships among variables change with respect to each other through time  
121 depending on system state (specific location on the attractor)—from time-series  
122 observations. Like a set of equations, the attractor encompasses the dynamics of a  
123 system, and thus can provide a mechanistic understanding of the system that is  
124 derived empirically, without requiring an *a priori* assumed set of equations.

125           Here, we used EDM and a proxy for susceptible population size (Rypdal &  
126 Sugihara 2019) to answer three questions: (1) Do temperature, rainfall, and/or  
127 inferred susceptible availability drive population-level dengue incidence? (2) Can  
128 we predict dengue dynamics using temperature and rainfall data and inferred  
129 susceptible availability? (3) What is the functional form of each climate–dengue  
130 relationship at the population level, and how is this relationship influenced by  
131 susceptible availability?

## 132 **METHODS**

### 133 **Time series data**

134 We obtained time series of weekly observations of dengue incidence (total number  
135 of new cases of all serotypes), average temperature (°C), and total rainfall (mm) in  
136 San Juan, Puerto Rico, for 19 seasons (1990/1991–2008/2009) spanning calendar  
137 week 18, 1990 to week 17, 2009 (Figure 1a–c) from the National Oceanic and  
138 Atmospheric Administration in November 2016  
139 (<http://dengueforecasting.noaa.gov/>). We obtained data for four additional seasons  
140 (2009/2010–2012/2013) from Johnson *et al.* (2018) in April 2020  
141 (<https://github.com/lrjohnson0/vbdcast>). Although dengue incidence data were  
142 also available for Iquitos, Peru (Johansson *et al.* 2019), we chose to focus on San  
143 Juan because the time series was longer, and therefore more amenable to EDM  
144 analyses (Munch *et al.* 2020).

145 Direct measurements of susceptible availability are not available, so from  
146 weekly incidence data  $I(t)$ , we estimated time-dependent growth rates:  $\lambda =$   
147  $I(t + \Delta t) / I(t)$ . The growth rate,  $\lambda$ , is proportional to the effective reproduction  
148 number,  $R_{\text{eff}}$ , and equivalent to  $R_{\text{eff}}$  if  $\Delta t$  equals the average time between primary  
149 and secondary host infections. Vector-borne disease models show that  $R_{\text{eff}}$  is  
150 proportional to the geometric mean of the susceptible host population and the  
151 susceptible vector population:  $R_{\text{eff}} = \sqrt{S_h S_v} R_0$ , where  $R_0$  is the basic reproduction  
152 number (Zhao *et al.* 2020). Hence,  $\lambda \propto \sqrt{S_h S_v}$  and  $\lambda$  can be used as a proxy for the  
153 susceptible population size at least during inter-outbreak periods where the  
154 transmission rate and  $R_0$  can be assumed to vary very little (Rypdal & Sugihara  
155 2019).

156 We estimated  $\lambda$  by linear regression using the model  $I(t + \Delta t) = \lambda I(t)$  for  
157 12 time points in a 12-week running window ( $\Delta t = 1$  week). The model is robust to  
158 the window size (Rypdal & Sugihara 2019). In the discrete case, when  $\lambda < 1$  the  
159 system is stable (inter-outbreak period) and when  $\lambda \geq 1$  then the system is unstable  
160 (outbreak period) (Supporting Information). We treated the resulting time series of  
161  $\lambda$ , hereafter “susceptibles index” (Figure 1d), as a proxy for the susceptible  
162 population size when  $\lambda < 1$ , and a proxy for the combined effects of susceptible  
163 availability and  $R_0$  when  $\lambda \geq 1$ .



## 164 **Empirical dynamic modeling (EDM)**

165 EDM infers a system's mechanistic underpinnings and predicts its dynamics using  
166 time series data of one or more variables to construct an attractor in state space  
167 (Figure S1). This procedure is called univariate (using lagged versions of a single  
168 variable time series) or multivariate state-space reconstruction (SSR). Properties of  
169 the attractor are assessed to examine characteristics of the system (Deyle &  
170 Sugihara 2011). We normalized each time series to zero mean and unit variance to  
171 remove measurement unit bias, ensuring the variables would be comparable and  
172 the attractor would not be distorted. All analyses were conducted in R version 3.5.1  
173 (R Development Core Team 2018) and all EDM analyses were performed using  
174 package *rEDM* (Park *et al.* 2020).

175 To infer mechanisms, EDM should be applied in systems where there is  
176 evidence of underlying low-dimensional deterministic dynamics (Cummins *et al.*  
177 2015). EDM assumptions are met when stochasticity is present (e.g., due to  
178 measurement noise, stochastic drivers, or unexplained variability) (Cenci *et al.*  
179 2019; Munch *et al.* 2020), but the system cannot be entirely stochastic. To test for  
180 low-dimensional deterministic dynamics we performed univariate SSR for each  
181 variable, and used *simplex projection* (Sugihara & May 1990)—a type of nearest  
182 neighbor regression performed on an attractor—to check whether the system is  
183 forecastable beyond the skill of an autoregressive model—an indicator of  
184 underlying deterministic dynamics (Figures S2a and S4; Supporting Information).  
185 To test for nonlinear state dependence of a variable—the motivation behind EDM—

186 we used the *S-map* test for nonlinearity (Sugihara 1994) (Figures S2b, c and S5;  
187 Supporting Information).

### 188 **EDM—Convergent cross-mapping**

189 We used an EDM approach called *convergent cross-mapping* (CCM) (Sugihara *et al.*  
190 2012) to identify drivers of dengue incidence. If two variables are causally related,  
191 then a multivariate attractor—where each variable in the system represents a  
192 dimension that traces the dynamics of the system—can be reconstructed (up to a  
193 practical limit) using lagged versions of just one of the variables (Figure S1). Based  
194 on Takens’ Theorem, this univariate “shadow attractor” preserves the structural and  
195 dynamic properties of the original multivariate attractor (Takens 1981; Sugihara *et*  
196 *al.* 2012). The concept behind CCM is that if temperature causes dengue incidence,  
197 then information about past temperature will be embedded in the dynamics of  
198 dengue, such that the shadow attractor produced using only incidence data allows  
199 us to accurately reconstruct temperature in the past. However, the converse  
200 scenario would not be true: since dengue does not cause temperature, the shadow  
201 attractor constructed using temperature data should not contain information to  
202 accurately reconstruct past dengue incidence (Supporting Information).

203         The critical criterion for estimating causal (directional) associations between  
204 two variables using CCM is checking that the cross-mapping skill (i.e., Pearson’s  
205 correlation coefficient,  $\rho$ , between predicted driver values using the univariate SSR  
206 of the response variable, and the observed driver values) monotonically increases

207 and plateaus (i.e., converges) with the length of the response variable time series  
208 used in cross-mapping. We used the Kendall's  $\tau$  test as a significance test for  
209 convergence of cross-mapping skill using the Kendall package (McLeod 2011). If  
210  $\tau > 0$  then there is convergence (Grziwotz *et al.* 2018).

211 We performed pairwise cross-correlations on the time series to investigate  
212 time-lagged relationships between potential drivers (i.e., temperature, rainfall, and  
213 susceptibles index) and dengue incidence using the `tseries` package (Trapletti &  
214 Hornik 2018). Based on these analyses (Figure S6), we applied a 9-week time lag  
215 between temperature and incidence, an averaged lag of 3–9 weeks for rainfall (i.e.,  
216 the average rainfall over the preceding 3–9 weeks) to resemble standing water as  
217 mosquito breeding habitat over a longer time period, and a 5-week lag for the  
218 susceptibles index. These lags are proxies for the time delays of potential cause-and-  
219 effects and are consistent with results from field studies (Chen *et al.* 2010; Stewart  
220 Ibarra *et al.* 2013).

221 We assessed the strength of evidence for effects of potential drivers on  
222 dengue by comparing the CCM performance using the data with the performance of  
223 two null models that control for the seasonal trend (i.e., interannual mean) observed  
224 in all variables (Figure 2). These null models address the sensitivity of CCM to  
225 periodic fluctuations (i.e., seasonality), which can make two variables appear to be  
226 causally linked when instead they are simply synchronized by a seasonal  
227 confounder (Cobey & Baskerville 2016; Deyle *et al.* 2016a). In the first “seasonal”  
228 null model, we preserved the seasonal signal, but randomized the interannual

229 anomalies (Deyle *et al.* 2016a). In the second, more conservative “Ebisuzaki” null  
230 model, we conserved any periodicity (beyond seasonal) and randomized the phases  
231 of Fourier-transformed time series (Ebisuzaki 1997). We tested for statistically  
232 significant differences in cross-mapping skill between the model that used the data  
233 *versus* the null models by performing Kolmogorov-Smirnov (K-S) tests after  
234 convergence.

235         We also repeated CCM in the nonsensical, reverse-causal direction (e.g., to  
236 test whether incidence drives climate) as a control for potential spurious  
237 relationships generated by non-causal covariation (e.g., due to seasonality). This  
238 addresses the issue of synchrony, in which CCM can indicate bidirectional causality  
239 when one direction is false or nonsensical (Baskerville & Cobey 2017; Sugihara *et al.*  
240 2017).

#### 241 **EDM—Forecast improvement**

242 We examined the predictive power of the drivers on dengue incidence by assessing  
243 how well we can predict dengue dynamics using temperature, rainfall, susceptibles  
244 index, and their combined effects. We used a combination of univariate SSR (i.e.,  
245 with incidence data) and multivariate SSR to build forecasting models and to  
246 determine the improvement of forecasting using simplex projection when including  
247 different combinations of drivers (Dixon *et al.* 1999; Deyle *et al.* 2013, 2016a)  
248 (Supporting Information). We built the SSR forecasting models/attractors using the

249 1990/1991–2008/2009 season data (Figure 1) and made forecasts 8 weeks ahead.

250 We assessed model forecasting performance using leave-one-out cross-validation.

251 Next, we evaluated out-of-sample forecasting performance of these models

252 using testing data from four additional seasons (2009/2010–2012/2013).

253 Predictions made on week zero for the first forecast of the 2009/2010–2012/2013

254 period (8 weeks ahead) came only from SSR using the 1990/1991–2008/2009 data.

255 All subsequent weekly forecasts (8 weeks ahead) were made from updated SSR

256 using all previous data, including past observations from the testing dataset.

257 Forecast uncertainty was evaluated by taking the density and morphology of

258 the attractor into account. The more compact a simplex was and the less its starting

259 position on the attractor mattered for the simplex projection, the more certain we

260 were about our point estimate. Forecast variance was obtained from a distribution

261 of weighted nearest neighbor regression from edges of simplexes constructed at

262 various starting positions in the past.

263 Finally, we compared our top model performance with performance of

264 previous models from 16 teams that participated in a dengue forecasting challenge

265 (Johansson *et al.* 2019) and had access to the same data. To make a fair comparison,

266 we followed the procedure as directed in the challenge (Supporting Information).

## 267 **EDM—Scenario exploration**

268 In nonlinear systems, drivers generally have an effect that is state-dependent: the  
269 strength and direction of the effect depends on the current state of the system.  
270 Scenario exploration with multivariate EDM allowed us to assess the effect of a  
271 small change in temperature or rainfall on dengue incidence, across different states  
272 of the system. The outcome of these small changes allowed us to deduce the  
273 relationship between each climate driver and dengue incidence and how they  
274 depend on the system state. For each time step  $t$  we used S-maps (Sugihara 1994;  
275 Deyle *et al.* 2016a) to predict dengue incidence using a small increase ( $+\Delta X$ ) and a  
276 small decrease ( $-\Delta X$ ) of the observed value of driver  $X(t)$  (temperature or rainfall).  
277 For each putative climate driver, the difference in dengue predictions between these  
278 small changes is  $\Delta Y = Y(t + 1) \left[ X(t) + \frac{\Delta X(t)}{2} \right] - Y(t + 1) \left[ X(t) - \frac{\Delta X(t)}{2} \right]$ , where  $Y(t +$   
279  $1)$  is a function of  $X$  and all other state variables, and we used  $\Delta Y/\Delta X$  to approximate  
280 the effect of driver  $X$  at time  $t$ . We repeated this over all time steps in our time series  
281 for both temperature and rainfall to recover their approximate relationships with  
282 dengue incidence at different states of the system. Scenario exploration analyses  
283 were repeated across several model parameterizations to address potential  
284 sensitivity to parameter settings (Supporting Information).

## 285 **RESULTS**

### 286 **Drivers of dengue dynamics**

287 EDM showed that temperature, rainfall, and the susceptibles index drive dengue  
288 incidence since the convergence criterion was met (Kendall's  $\tau > 0$ ,  $P < 0.01$ ) in all  
289 three cases (Figure 3a–c). Rainfall and susceptibles index were significant drivers of  
290 dengue incidence beyond seasonality, as their effects were distinguishable from  
291 seasonal and Ebisuzaki null models (Figures 3b–c and S8b–c; K-S  $P < 0.0001$ ). This  
292 implies statistically significant effects of both rainfall and the susceptibles index on  
293 dengue, which are not obscured by a periodic confounder. However, temperature  
294 was not a significant driver beyond seasonality (Figures 3a and S8a; K-S  $P = 0.90$ ).  
295 We cannot rule out the possibility that the apparent forcing of temperature on  
296 dengue is due to a seasonal confounder. However, if no such confounder exists, then  
297 the seasonal trend in temperature, which accounts for most temperature variation  
298 in San Juan, drives the seasonal trend observed in dengue incidence. Compared to  
299 the other drivers, the converging cross-mapping skill of the temperature null  
300 models were relatively high (Figures 3 and S8), suggesting that temperature  
301 seasonality in each null model was a strong driver. Thus, seasonal temperature may  
302 be driving dengue dynamics, a result consistent with other studies (Huber *et al.*  
303 2018; Robert *et al.* 2019).

304 As expected, EDM tests for putative causality in the nonsensical directions—  
305 incidence driving temperature or rainfall—were not significant (i.e., no

306 convergence; Figure S7, black lines). This result further supports the finding that  
307 temperature and rainfall drive dengue incidence, because their causal relationships  
308 were not confounded by spurious bidirectionality. The null models for the  
309 nonsensical directions of causality (Figure S7, grey lines) also displayed no  
310 convergence (completely flat), as expected (i.e., seasonality of dengue incidence  
311 does not drive seasonality of temperature or rainfall). However, seasonality (or any  
312 periodicity) of temperature, rainfall and susceptibles index drive dengue dynamics,  
313 shown by convergence of the seasonal and Ebisuzaki null models (grey lines in  
314 Figures 3 and S8).

### 315 **Predictive power of drivers**

316 The multivariate SSR model using only temperature and rainfall data did not predict  
317 dengue incidence very well ( $\rho = 0.3839$ , RMSE = 47.72) although it captured the  
318 seasonality of the epidemics (Figure 4a). Forecasting skill doubled when the  
319 susceptibles index was included along with rainfall and temperature ( $\rho = 0.7547$ ,  
320 RMSE = 37.40; Figure 4c), where timing and magnitude of epidemics were captured  
321 reasonably well. Dengue incidence prediction improved even further when  
322 incidence was added into the model with all drivers ( $\rho = 0.7662$ , RMSE = 37.14;  
323 Figure 4e). Dengue incidence was somewhat predictable using univariate SSR of  
324 incidence data alone ( $\rho = 0.4459$ , RMSE = 46.75; Figure 4g), suggesting that the  
325 dengue incidence time series contains information about its drivers, although  
326 limited. This points to some additional value of including the driver variables.



327 We also evaluated the performance of the SSR models (Figure 4a, c, e, g)  
328 constructed using data from seasons 1990/1991–2008/2009 on external, testing  
329 data from 2009/2010–2012/2013 that were not used in SSR (Figure 4b, d, f, h). The  
330 average out-of-sample forecasting skill for each model for the testing seasons was  
331 higher than that of the 1990/1991–2008/2009 forecasts, although the errors were  
332 larger. The model using only temperature and rainfall displayed predictability ( $\rho =$   
333 0.8989, RMSE = 52.30; Figure 4b), the model that also included the susceptibles  
334 index improved predictions ( $\rho = 0.9475$ , RMSE = 52.12; Figure 4d), and the model  
335 that also included past incidence made highly accurate predictions ( $\rho = 0.9697$ ,  
336 RMSE = 46.75; Figure 4f). The model that only included dengue incidence without  
337 the drivers was also predictive, although more error-prone ( $\rho = 0.9044$ , RMSE =  
338 57.34; Figure 4h). All SSR models (Figure 4a–h) had significant forecasting skill ( $\rho$ )  
339 values (Fisher's z-transformation  $P < 0.001$ ).

340 The model with the highest prediction skill for the testing seasons  
341 (2009/2010–2012/2013), which included past climate, susceptibles index, and  
342 incidence data as predictors (Figure 4f), also outperformed models from the dengue  
343 forecasting challenge, including the ensemble model (Johansson *et al.* 2019) for  
344 predicting peak incidence, peak week, and seasonal incidence for all seasons on  
345 average (Tables S1–S2, Figures S9–S12). This demonstrates the benefit of the EDM  
346 approach for capturing the mechanistic, nonlinear, interdependent relationships  
347 among drivers over both equation-based mechanistic models and phenomenological  
348 models.

## 349 **State-dependent functional responses**

350 As expected, we find state-dependent effects of temperature and rainfall with non-  
351 zero median effects. We found that temperature had a small positive median effect  
352 (2.88 cases/°C, Wilcox  $P < 0.001$ ) on dengue incidence (Figure 5a). A positive effect  
353 is expected for the temperature range in Puerto Rico (Mordecai *et al.* 2017) (Figure  
354 6e, black dashed lines), although the effect was occasionally much stronger, both  
355 positive and negative (Figure 5a, b). The large negative effects occurred only at the  
356 highest temperature values (as predicted by mechanistic models of temperature-  
357 dependent transmission), reinforced by a lower quantile regression with a strongly  
358 negative slope (Figure 5b, bottom dashed red line). However, positive effects  
359 occurred across the whole temperature range, which is limited to temperatures  
360 below the 29°C optimal temperature for transmission estimated from mathematical  
361 models and laboratory data (Mordecai *et al.* 2017).

362         Rainfall had a small negative median effect (−0.12 cases/mm, Wilcox  $P <$   
363 0.001), but occasionally had very large negative effects (Figure 5a, c). These large,  
364 negative effects of rainfall on dengue occurred when there was less than 100 mm of  
365 rain per week (Figure 5c), consistent with expectations that drought could lead to a  
366 high number of dengue cases due to water storage, which can provide mosquito  
367 breeding habitat (Oliveira-lima *et al.* 2000). There are also small positive effects of  
368 rainfall on dengue (Figure 5c), suggesting that overall the results showed competing  
369 effects of low to moderate rain providing standing water for mosquito breeding and

370 humans storing water where mosquitoes can breed when there is drought or low  
371 rainfall.

372         These results suggest the strength and direction of the effects of climate on  
373 dengue dynamics depend on the state of the system. In addition to the nonlinear  
374 effects of climate drivers themselves on dengue incidence, another potential cause  
375 of state-dependent climate effects on dengue dynamics is the variation in the  
376 susceptible population size over time (Figure 6a, b). Outbreaks do not occur when  
377 there are too few susceptible people in the population. As expected, when the  
378 susceptibles index was small ( $\lambda < 0.85$ ) incidence was insensitive to climate (Figure  
379 6c, f). By contrast, when the susceptibles index was large ( $\lambda > 0.85$ ), temperature  
380 and rainfall effects on dengue incidence appeared (Figure 6d, g). The gradual  
381 increase and decrease of the rate of change of dengue as a function of temperature  
382 (Figure 6d, red solid lines) aligned well with the changes in slope over the  
383 increasing part (Figure 6e, black dashed lines representing the temperature range in  
384 our study) of the unimodal temperature response curve for dengue transmission by  
385 *Ae. aegypti* developed previously (Mordecai *et al.* 2017). This is an important  
386 finding, since evidence of climate functional responses for disease dynamics is rare  
387 due to the difficulty of obtaining appropriately informative field data. It is possible  
388 that if we had temperature data ranging across a larger spectrum—possibly by  
389 assembling data across multiple climates—that the empirical functional response  
390 derived from EDM would also look unimodal. Further, when the susceptibles index  
391 was high, the slope of the relationship between rainfall and dengue incidence  
392 became more negative as rainfall increased, suggesting a concave-down effect of

393 rainfall on incidence (Figure 6g, h). This relationship has been difficult to  
394 characterize in the field because of multiple, possibly context-dependent and lagged,  
395 mechanisms linking rainfall to dengue.

## 396 **DISCUSSION**

397 High host susceptibility allows seasonal climate suitability to fuel large dengue  
398 epidemics in San Juan, Puerto Rico. The effects of climate and susceptibility are  
399 nonlinear, interdependent, and state-dependent, which makes inference from  
400 controlled mechanistic experiments, equation-based mechanistic models, or  
401 phenomenological models difficult. EDM provides an essential toolkit for identifying  
402 these drivers, quantifying their predictive power, and approximating their  
403 functional responses. In Puerto Rico, the causes of extensive interannual variability  
404 in dengue incidence have remained a mystery, despite hypotheses that climate and  
405 host susceptibility were involved. Here, we used EDM and a proxy for susceptible  
406 availability to disentangle nonlinear and interactive mechanisms driving disease  
407 dynamics.

408         We found that rainfall, susceptible availability, and plausibly temperature  
409 (via its seasonality) interact to drive dengue incidence. Combined, these three  
410 drivers predicted dengue incidence with high accuracy (Figure 4c). The EDM-based  
411 forecasting model outperformed 16 models and an ensemble model in a recently  
412 published dengue forecasting challenge (Johansson *et al.* 2019), suggesting that it  
413 could enhance dengue control efforts if surveillance efforts continue to report

414 weekly case data. Finally, as expected from epidemiological theory, climate effects  
415 on dengue only appeared when susceptible availability exceeded a threshold ( $\lambda >$   
416 0.85; Figure 6).

417         The fact that climate effects are first observed when  $\lambda \approx 0.85$  (before the  
418 onset of an outbreak,  $\lambda = 1$ ), suggests that rainfall, and possibly temperature, have  
419 an effect on the timing of an impending epidemic. Climate could drive the  
420 transmission rate, thus influencing  $\lambda$  (which is proportional to both susceptible  
421 population size and  $R_0$  when  $\lambda$  is close to 1), and therefore the timing of an outbreak  
422 could be attributed to the changes in transmission caused by seasonal climatic  
423 drivers (Rypdal & Sugihara 2019). The seasonality of temperature and rainfall had  
424 higher predictive skill than seasonality of susceptibles index (Figures 3 and S8, grey  
425 lines), further supporting that seasonality of incidence was associated with climate.  
426 However, the susceptibles index was critical for predicting dengue epidemic  
427 magnitudes (Figure 4c-f). Using the same data, Johnson *et al.* (2018) found that  
428 mechanistic models could predict the timing of seasonal epidemics, but that a  
429 phenomenological machine learning component was needed to capture interannual  
430 variation in epidemic magnitude. Our work suggests that the unobserved size of the  
431 susceptible population was a key missing link for predicting magnitude variation  
432 across years.

433         Previous studies have built models accounting for both susceptible  
434 availability and climate on dengue by reconstructing time series of susceptibles  
435 from a compartmental modeling framework (Metcalf *et al.* 2017). However, no

436 previous studies on dengue have explored the interdependence between climate  
437 and susceptible population size. We showed that susceptible availability modifies  
438 climate effects on dengue: climate has negligible effects unless the susceptible  
439 population size is large enough (Figure 6). The interdependence of climate and  
440 population susceptibility has also been studied in diseases where the opposite effect  
441 was found. For example, climate effects on SARS-CoV-2 are expected to be negligible  
442 when susceptible availability is high in the early stage of the emerging pandemic  
443 (Baker *et al.* 2020). For influenza dynamics, population density in cities—potentially  
444 a proxy for susceptible availability—also modulated climate effects on disease  
445 transmission: climate effects were negligible in cities with high population densities  
446 (Dalziel *et al.* 2018).

447       Because dengue susceptibility is so complex—due to the serotype dynamics  
448 and time- and antibody titer-dependent cross-protection and enhancement  
449 (Katzelnick *et al.* 2017b)—total population density or size may not be a reasonable  
450 proxy for susceptible availability in dengue dynamics, and a direct mechanistic  
451 estimate of population susceptibility will likely never be widely available for most  
452 populations. Accordingly, it has been difficult for previous mechanistic models to  
453 capture susceptible dynamics for dengue and their interactions with climate.  
454 However, our approach provides a useful proxy that captures the susceptible  
455 population dynamics even in the absence of more detailed immunological  
456 information. By inferring the susceptibles index from incidence data, we were able  
457 to capture the strong influence of the susceptible availability on dengue dynamics,  
458 which in turn moderated the effect of climate on dengue dynamics. This result is

459 expected from theory (Kermack & McKendrick 1927; Xu *et al.* 2017), but  
460 demonstrating it empirically is a unique contribution of this study.

461 Even when accounting for susceptible availability, the effects of temperature  
462 and rainfall on dengue were strongly state-dependent (Figure 6d, g). This result is  
463 potentially due to nonlinear effects of each climate driver (Figure 6e, h), interactions  
464 and correlations between temperature and rainfall, microclimate variation over  
465 space and time that is not captured by weekly averages, and complex lagged effects  
466 that are not captured by a single fixed lag (e.g., 9 weeks). In Puerto Rico, mosquitoes  
467 also breed in septic tanks year-round, allowing transmission to occur independently  
468 from rainfall (Mackay *et al.* 2009), thus weakening the rainfall–dengue negative  
469 relationship (Figure 6g). Some of this additional variation may be captured in the  
470 dengue incidence time series itself, which may explain why including it improves  
471 forecast skill over climate and susceptibility alone (Figure 4e, f). Despite this  
472 additional variation, our results are consistent with previous studies suggesting that  
473 dengue dynamics in Puerto Rico are positively associated with temperature  
474 (Johansson *et al.* 2009b; Barrera *et al.* 2011; Morin *et al.* 2015), and possibly  
475 negatively associated with rainfall (Johansson *et al.* 2009a; Morin *et al.* 2015), since  
476 most *Ae. aegypti* pupae in Puerto Rico are produced in human-made containers  
477 during periods of drought (Barrera *et al.* 2011).

478 The climate and incidence data used here have been used in multiple  
479 forecasting efforts, where ensemble approaches and approaches that incorporated  
480 mechanisms outperformed purely statistical approaches (Johansson *et al.* 2019).

481 However, even the high-performing forecasting methods using the same dataset,  
482 and including (experimentally-derived) assumed mechanisms for the joint influence  
483 of climate and susceptibility on dengue dynamics, are still error-prone to the timing  
484 (on the order of weeks) and the magnitude (on the order of 50 cases) of intra-  
485 annual epidemics (Morin *et al.* 2015; Johansson *et al.* 2019). Mechanisms isolated  
486 independently in controlled experiments do not necessarily scale up to the  
487 population level, and susceptible dynamics derived from compartmental models  
488 may be too simple to properly capture true susceptibility at the population level for  
489 dengue (Katzelnick *et al.* 2017b). EDM allowed us to infer mechanisms empirically  
490 from population-level data, and accounted for the population-level interdependence  
491 between climate and susceptible availability for forecasting, which probably  
492 contributed to our model outperforming previous forecasting models and  
493 ensembles (Table S1).

494         Connecting climate and dengue at the population level is challenging,  
495 because causal relationships are likely to be nonlinear and state-dependent. A  
496 toolkit of methods for testing hypotheses, understanding mechanisms, and making  
497 predictions is essential for understanding disease dynamics in complex, natural  
498 populations. Ultimately, understanding how climate-driven vector-borne diseases  
499 are influenced by other variables, such as susceptible population size, is important  
500 for optimizing vector control under critical conditions where climate might spark  
501 epidemics. Our approach, using EDM and an inferred proxy for the susceptible  
502 population size from data, confirmed that climate has nonlinear, seasonal effects on  
503 dengue epidemics in San Juan, Puerto Rico, but only above a certain threshold of



504 susceptible availability. The mechanisms inferred from EDM could be applied to  
505 understand and predict future ecological responses to changing environments,  
506 including dengue epidemics in a world undergoing rapid environmental change.

## 507 **ACKNOWLEDGEMENTS**

508 We thank Giulio De Leo, Marcus Feldman, Dmitri Petrov, and members of the  
509 Fukami, Mordecai, Peay, and Sugihara labs for helpful feedback. NN was supported  
510 by the Bing Fellowship in Honor of Paul Ehrlich and the Stanford Data Science  
511 Scholars program. ERD and GS were supported by the National Science Foundation  
512 (NSF) DEB-1655203, NSF-ABI-1667584, DoD-Strategic Environmental Research and  
513 Development Program (SERDP) 15 RC-2509; Lenfest Foundation Award 00028335  
514 and the McQuown Chair in Natural Sciences, University of California, San Diego. MSS  
515 and EAM were supported by an NSF Ecology and Evolution of Infectious Diseases  
516 grant (DEB-1518681). EAM was also supported by an NSF Rapid Response Research  
517 grant (RAPID 1640780), an NIH NIGMS R35 MIRA award (R35GM133439), the  
518 Stanford University Woods Institute for the Environment Environmental Ventures  
519 Program, the Hellman Faculty Fellowship, a Stanford King Center Seed Grant, and  
520 the Terman Fellowship. AJM was supported by an NSF Postdoctoral Research  
521 Fellowship in Biology (1611767). MLC was supported by the Lindsay Family E-IPER  
522 Fellowship and Illich-Sadowsky Interdisciplinary Graduate Fellowship.

523 **REFERENCES**

- 524 Anderson, R.M. & May, R.M. (1979). Population biology of infectious diseases: Part I.  
525 *Nature*, 280, 361–367.
- 526 Baker, R.E., Yang, W., Vecchi, G.A., Metcalf, C.J.E. & Grenfell, B.T. (2020). Susceptible  
527 supply limits the role of climate in the early SARS-CoV-2 pandemic. *Science*,  
528 369, 315–319.
- 529 Barrera, R., Amador, M. & MacKay, A.J. (2011). Population dynamics of *Aedes*  
530 *egypti* and dengue as influenced by weather and human behavior in san juan,  
531 puerto rico. *PLoS Negl. Trop. Dis.*, 5, e1378.
- 532 Baskerville, E.B. & Cobey, S. (2017). Does influenza drive absolute humidity? *Proc.*  
533 *Natl. Acad. Sci.*, 114, 201700369.
- 534 Brady, O.J., Gething, P.W., Bhatt, S., Messina, J.P., Brownstein, J.S., Hoen, A.G., *et al.*  
535 (2012). Refining the Global Spatial Limits of Dengue Virus Transmission by  
536 Evidence-Based Consensus. *PLoS Negl. Trop. Dis.*, 6, e1760.
- 537 Caldwell, J., LaBeaud, D., Lambin, E., Stewart-Ibarra, A., Ndenga, B., Mutuku, F., *et al.*  
538 (2020). Climate explains geographic and temporal variation in mosquito-borne  
539 disease dynamics on two continents. *bioRxiv*, 2020.02.07.938720.
- 540 Cenci, S., Sugihara, G. & Saavedra, S. (2019). Regularized S-map for inference and  
541 forecasting with noisy ecological time series. *Methods Ecol. Evol.*, 2041–  
542 210X.13150.
- 543 Chen, S.C., Liao, C.M., Chio, C.P., Chou, H.H., You, S.H. & Cheng, Y.H. (2010). Lagged

- 544 temperature effect with mosquito transmission potential explains dengue  
545 variability in southern Taiwan: Insights from a statistical analysis. *Sci. Total*  
546 *Environ.*, 408, 4069–4075.
- 547 Cobey, S. & Baskerville, E.B. (2016). Limits to causal inference with state-space  
548 reconstruction for infectious disease. *PLoS One*, 11, 1–22.
- 549 Cummins, B., Gedeon, T. & Spendlove, K. (2015). On the Efficacy of State Space  
550 Reconstruction Methods in Determining Causality. *SIAM J. Appl. Dyn. Syst.*, 14,  
551 335–381.
- 552 Dalziel, B.D., Kissler, S., Gog, J.R., Viboud, C., Bjørnstad, O.N., Metcalf, C.J.E., *et al.*  
553 (2018). Urbanization and humidity shape the intensity of influenza epidemics  
554 in U.S. cities. *Science*, 362, 75–79.
- 555 Deyle, E.R., Fogarty, M., Hsieh, C., Kaufman, L., Maccall, A.D. & Munch, S.B. (2013).  
556 Predicting climate effects on Pacific sardine. *Proc. Natl. Acad. Sci. U. S. A.*, 110,  
557 6430–6435.
- 558 Deyle, E.R., Maher, M.C., Hernandez, R.D., Basu, S. & Sugihara, G. (2016a). Global  
559 environmental drivers of influenza. *Proc. Natl. Acad. Sci.*, 113, 13081–13086.
- 560 Deyle, E.R., May, R.M., Munch, S.B. & Sugihara, G. (2016b). Tracking and forecasting  
561 ecosystem interactions in real time. *Proc. R. Soc. B Biol. Sci.*, 283.
- 562 Deyle, E.R. & Sugihara, G. (2011). Generalized theorems for nonlinear state space  
563 reconstruction. *PLoS One*, 6.
- 564 Dixon, P.A., Milicich, M.J. & Sugihara, G. (1999). Episodic fluctuations in larval supply.  
565 *Science*, 283, 1528–1530.

- 566 Dushoff, J., Plotkin, J.B., Levin, S.A. & Earn, D.J.D. (2004). Dynamical resonance can  
567 account for seasonality of influenza epidemics. *Proc. Natl. Acad. Sci. U. S. A.*, 101,  
568 16915–16916.
- 569 Ebisuzaki, W. (1997). A method to estimate the statistical significance of a  
570 correlation when the data are serially correlated. *J. Clim.*, 10, 2147–2153.
- 571 Erlanger, T.E., Keiser, J. & Utzinger, J. (2008). Effect of dengue vector control  
572 interventions on entomological parameters in developing countries: A  
573 systematic review and meta-analysis. *Med. Vet. Entomol.*
- 574 Gordon, A., Kuan, G., Mercado, J.C., Gresh, L., Avilés, W., Balmaseda, A., *et al.* (2013).  
575 The Nicaraguan Pediatric Dengue Cohort Study: Incidence of Inapparent and  
576 Symptomatic Dengue Virus Infections, 2004-2010. *PLoS Negl. Trop. Dis.*, 7,  
577 e2462.
- 578 Grziwotz, F., Strauß, J.F., Hsieh, C. & Telschow, A. (2018). Empirical Dynamic  
579 Modelling Identifies different Responses of *Aedes Polynesiensis* Subpopulations  
580 to Natural Environmental Variables. *Sci. Rep.*, 8, 16768.
- 581 Hamel, R., Surasombatpattana, P., Wichit, S., Dauvé, A., Donato, C., Pompon, J., *et al.*  
582 (2019). Phylogenetic analysis revealed the co-circulation of four dengue virus  
583 serotypes in Southern Thailand. *PLoS One*, 14, e0221179.
- 584 Hii, Y.L., Zhu, H., Ng, N., Ng, L.C. & Rocklöv, J. (2012). Forecast of Dengue Incidence  
585 Using Temperature and Rainfall. *PLoS Negl. Trop. Dis.*, 6, e1908.
- 586 Huber, J.H., Childs, M.L., Caldwell, J.M. & Mordecai, E.A. (2018). Seasonal  
587 temperature variation influences climate suitability for dengue, chikungunya,

- 588 and Zika transmission. *PLoS Negl. Trop. Dis.*, 12, e0006451.
- 589 Jiménez-Silva, C.L., Carreño, M.F., Ortiz-Baez, A.S., Rey, L.A., Villabona-Arenas, C.J. &  
590 Ocazionez, R.E. (2018). Evolutionary history and spatio-temporal dynamics of  
591 dengue virus serotypes in an endemic region of Colombia. *PLoS One*, 13,  
592 e0203090.
- 593 Johansson, M.A., Apfeldorf, K.M., Dobson, S., Devita, J., Buczak, A.L., Baugher, B., *et al.*  
594 (2019). An open challenge to advance probabilistic forecasting for dengue  
595 epidemics. *Proc. Natl. Acad. Sci.*, 116, 24268–24274.
- 596 Johansson, M.A., Cummings, D.A.T. & Glass, G.E. (2009a). Multiyear climate  
597 variability and dengue - El Niño southern oscillation, weather, and dengue  
598 incidence in Puerto Rico, Mexico, and Thailand: A longitudinal data analysis.  
599 *PLoS Med.*, 6, e1000168.
- 600 Johansson, M.A., Dominici, F. & Glass, G.E. (2009b). Local and global effects of climate  
601 on dengue transmission in Puerto Rico. *PLoS Negl. Trop. Dis.*, 3, e382.
- 602 Johansson, M.A., Reich, N.G., Hota, A., Brownstein, J.S. & Santillana, M. (2016).  
603 Evaluating the performance of infectious disease forecasts: A comparison of  
604 climate-driven and seasonal dengue forecasts for Mexico. *Sci. Rep.*, 6, 33707.
- 605 Johnson, L.R., Gramacy, R.B., Cohen, J., Mordecai, E., Murdock, C., Rohr, J., *et al.*  
606 (2018). Phenomenological forecasting of disease incidence using  
607 heteroskedastic gaussian processes: A dengue case study. *Ann. Appl. Stat.*, 12,  
608 27–66.
- 609 Katzelnick, L.C., Coloma, J. & Harris, E. (2017a). Dengue: knowledge gaps, unmet

- 610 needs, and research priorities. *Lancet Infect. Dis.*, 17, e88–e100.
- 611 Katzelnick, L.C., Gresh, L., Halloran, M.E., Mercado, J.C., Kuan, G., Gordon, A., *et al.*  
612 (2017b). Antibody-dependent enhancement of severe dengue disease in  
613 humans. *Science*, 358, 929–932.
- 614 Kermack, W.O. & McKendrick, A.G. (1927). A Contribution to the Mathematical  
615 Theory of Epidemics. *Proc. R. Soc. A Math. Phys. Eng. Sci.*, 115, 700–721.
- 616 Kilpatrick, A.M. & Randolph, S.E. (2012). Drivers, dynamics, and control of emerging  
617 vector-borne zoonotic diseases. *Lancet*.
- 618 Koenraadt, C.J.M. & Harrington, L.C. (2008). Flushing effect of rain on container-  
619 inhabiting mosquitoes *Aedes aegypti* and *Culex pipiens* (Diptera: *Culicidae*). *J.*  
620 *Med. Entomol.*, 45, 28–35.
- 621 Kraemer, M.U.G., Reiner, R.C., Brady, O.J., Messina, J.P., Gilbert, M., Pigott, D.M., *et al.*  
622 (2019). Past and future spread of the arbovirus vectors *Aedes aegypti* and *Aedes*  
623 *albopictus*. *Nat. Microbiol.*, 4, 854–863.
- 624 Kraemer, M.U.G., Sinka, M.E., Duda, K.A., Mylne, A.Q.N., Shearer, F.M., Barker, C.M., *et*  
625 *al.* (2015). The global distribution of the arbovirus vectors *Aedes aegypti* and  
626 *Ae. Albopictus*. *Elife*, 4.
- 627 Lambrechts, L., Paaijmans, K.P., Fansiri, T., Carrington, L.B., Kramer, L.D., Thomas,  
628 M.B., *et al.* (2011). Impact of daily temperature fluctuations on dengue virus  
629 transmission by *Aedes aegypti*. *Proc. Natl. Acad. Sci. U. S. A.*, 108, 1–6.
- 630 Liu-Helmersson, J., Stenlund, H., Wilder-Smith, A. & Rocklöv, J. (2014). Vectorial  
631 capacity of *Aedes aegypti*: Effects of temperature and implications for global

- 632 dengue epidemic potential. *PLoS One*, 9.
- 633 Mackay, A.J., Amador, M., Diaz, A., Smith, J. & Barrera, R. (2009). Dynamics of *Aedes*  
634 *aegypti* and *Culex quinquefasciatus* in Septic Tanks. *J. Am. Mosq. Control Assoc.*,  
635 25, 409–416.
- 636 McLeod, A.I. (2011). Kendall: Kendall rank correlation and Mann-Kendall trend test.
- 637 Metcalf, C.J.E., Walter, K.S., Wesolowski, A., Buckee, C.O., Shevliakova, E., Tatem, A.J.,  
638 *et al.* (2017). Identifying climate drivers of infectious disease dynamics: Recent  
639 advances and challenges ahead. *Proc. R. Soc. B Biol. Sci.*
- 640 Mina, M.J., Metcalf, C.J.E., De Swart, R.L., Osterhaus, A.D.M.E. & Grenfell, B.T. (2015).  
641 Long-term measles-induced immunomodulation increases overall childhood  
642 infectious disease mortality. *Science*, 348, 694–699.
- 643 Mordecai, E.A., Caldwell, J.M., Grossman, M.K., Lippi, C.A., Johnson, L.R., Neira, M., *et*  
644 *al.* (2019). Thermal biology of mosquito-borne disease. *Ecol. Lett.*, e13335.
- 645 Mordecai, E.A., Cohen, J.M., Evans, M. V., Gudapati, P., Johnson, L.R., Lippi, C.A., *et al.*  
646 (2017). Detecting the impact of temperature on transmission of Zika, dengue,  
647 and chikungunya using mechanistic models. *PLoS Negl. Trop. Dis.*, 11,  
648 e0005568.
- 649 Morin, C.W., Monaghan, A.J., Hayden, M.H., Barrera, R. & Ernst, K. (2015).  
650 Meteorologically driven simulations of dengue epidemics in San Juan, PR. *PLoS*  
651 *Negl. Trop. Dis.*, 9, e0004002.
- 652 Munch, S.B., Brias, A., Sugihara, G. & Rogers, T.L. (2020). Frequently asked questions  
653 about nonlinear dynamics and empirical dynamic modelling. *ICES J. Mar. Sci.*,

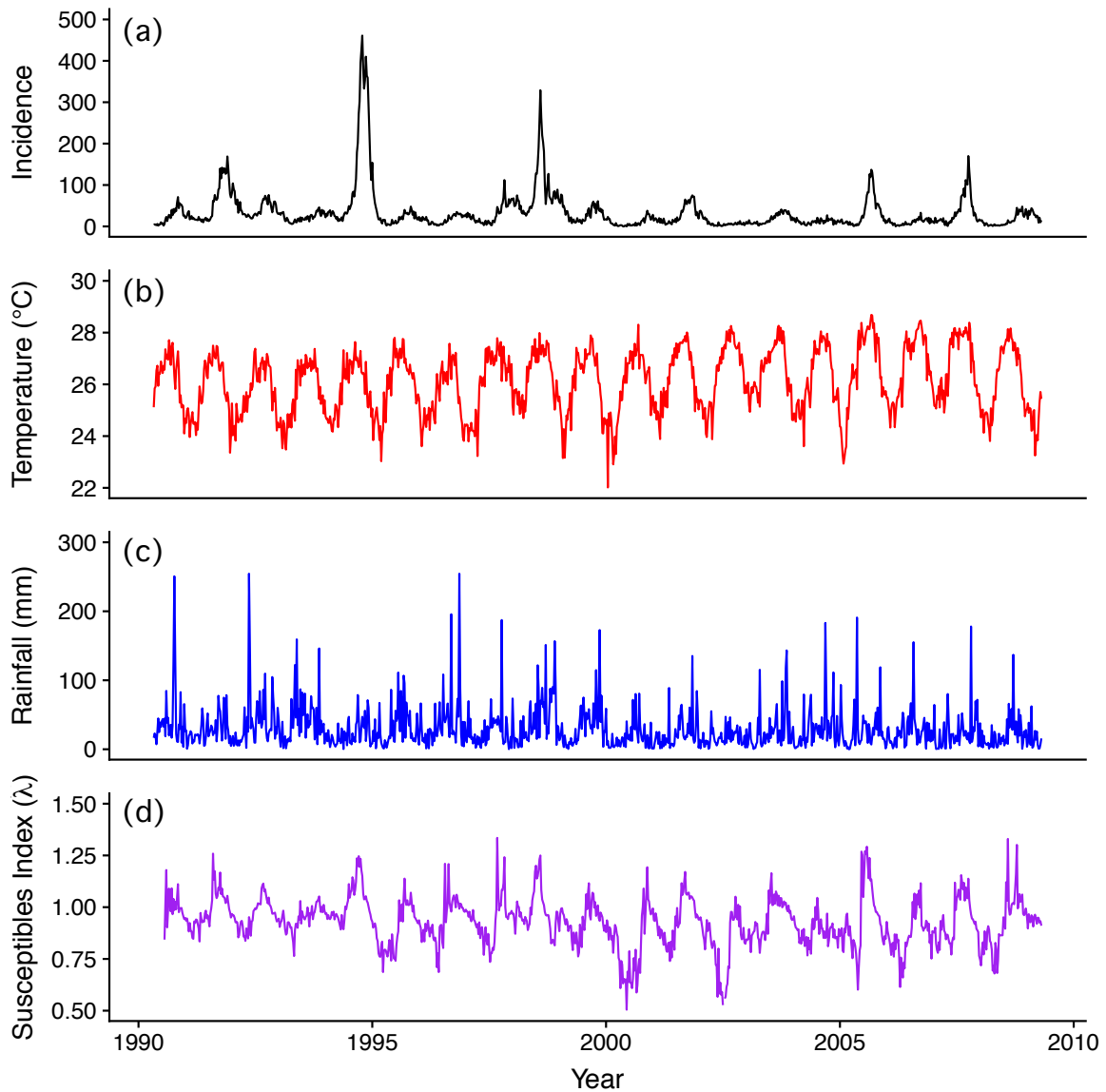


- 654 77, 1463–1479.
- 655 Oliveira-lima, W., Hodgson, J.C., Pontes, R.J.S. & Freeman, J. (2000). Vector densities  
656 that potentiate dengue outbreaks in a Brazilian city. *Trop. Med.*, 62, 378–383.
- 657 Park, J., Smith, C., Sugihara, G. & Deyle, E.R. (2020). rEDM: Empirical Dynamic  
658 Modeling ('EDM'). R package version 1.6.1.
- 659 Pitzer, V.E., Viboud, C., Alonso, W.J., Wilcox, T., Metcalf, C.J., Steiner, C.A., *et al.* (2015).  
660 Environmental Drivers of the Spatiotemporal Dynamics of Respiratory  
661 Syncytial Virus in the United States. *PLoS Pathog.*, 11, 1–14.
- 662 Robert, M.A., Christofferson, R.C., Weber, P.D. & Wearing, H.J. (2019). Temperature  
663 impacts on dengue emergence in the United States: Investigating the role of  
664 seasonality and climate change. *Epidemics*, 28.
- 665 Ryan, S.J., Carlson, C.J., Mordecai, E.A. & Johnson, L.R. (2019). Global expansion and  
666 redistribution of *Aedes*-borne virus transmission risk with climate change. *PLoS*  
667 *Negl. Trop. Dis.*, 13, e0007213.
- 668 Rypdal, M. & Sugihara, G. (2019). Inter-outbreak stability reflects the size of the  
669 susceptible pool and forecasts magnitudes of seasonal epidemics. *Nat.*  
670 *Commun.*, 10, 2374.
- 671 dos Santos, T.P., Cruz, O.G., da Silva, K.A.B., de Castro, M.G., de Brito, A.F., Maspero,  
672 R.C., *et al.* (2017). Dengue serotype circulation in natural populations of *Aedes*  
673 *aegypti*. *Acta Trop.*, 176, 140–143.
- 674 Sridhar, S., Luedtke, A., Langevin, E., Zhu, M., Bonaparte, M., Machabert, T., *et al.*  
675 (2018). Effect of Dengue Serostatus on Dengue Vaccine Safety and Efficacy. *N.*

- 676 *Engl. J. Med.*, 379, 327–340.
- 677 Stewart Ibarra, A.M., Ryan, S.J., Beltrá N, E., Mejía, R.L., Silva, M. & Muñ Oz, N. (2013).  
678 Dengue Vector Dynamics (*Aedes aegypti*) Influenced by Climate and Social  
679 Factors in Ecuador: Implications for Targeted Control. *PLoS One*, 8.
- 680 Sugihara, G. (1994). Nonlinear forecasting for the classification of natural time  
681 series. *Philos. Trans. R. Soc. A Math. Phys. Eng. Sci.*, 348, 477–495.
- 682 Sugihara, G., Deyle, E.R. & Ye, H. (2017). Reply to Baskerville and Cobey:  
683 Misconceptions about causation with synchrony and seasonal drivers. *Proc.*  
684 *Natl. Acad. Sci.*, 114, 201700998.
- 685 Sugihara, G., May, R., Ye, H., Hsieh, C., Deyle, E., Fogarty, M., *et al.* (2012). Detecting  
686 Causality in Complex Ecosystems. *Science*, 338, 496–500.
- 687 Sugihara, G. & May, R.M. (1990). Nonlinear forecasting as a way of distinguishing  
688 chaos from measurement error in time series. *Nature*, 344, 734–741.
- 689 Takens, F. (1981). Detecting strange attractors in turbulence. In: *Dynamical Systems*  
690 *and Turbulence, Warwick 1980, Lecture Notes in Mathematics* (eds. Rand, D. &  
691 Young, L.-S.). Springer, Berlin, Heidelberg., pp. 366–381.
- 692 Tran, A., L'Ambert, G., Lacour, G., Benoît, R., Demarchi, M., Cros, M., *et al.* (2013). A  
693 rainfall- and temperature-driven abundance model for *Aedes albopictus*  
694 populations. *Int. J. Environ. Res. Public Health*, 10, 1698–1719.
- 695 Trapletti, A. & Hornik, K. (2018). *tseries: Time Series Analysis and Computational*  
696 *Finance*.

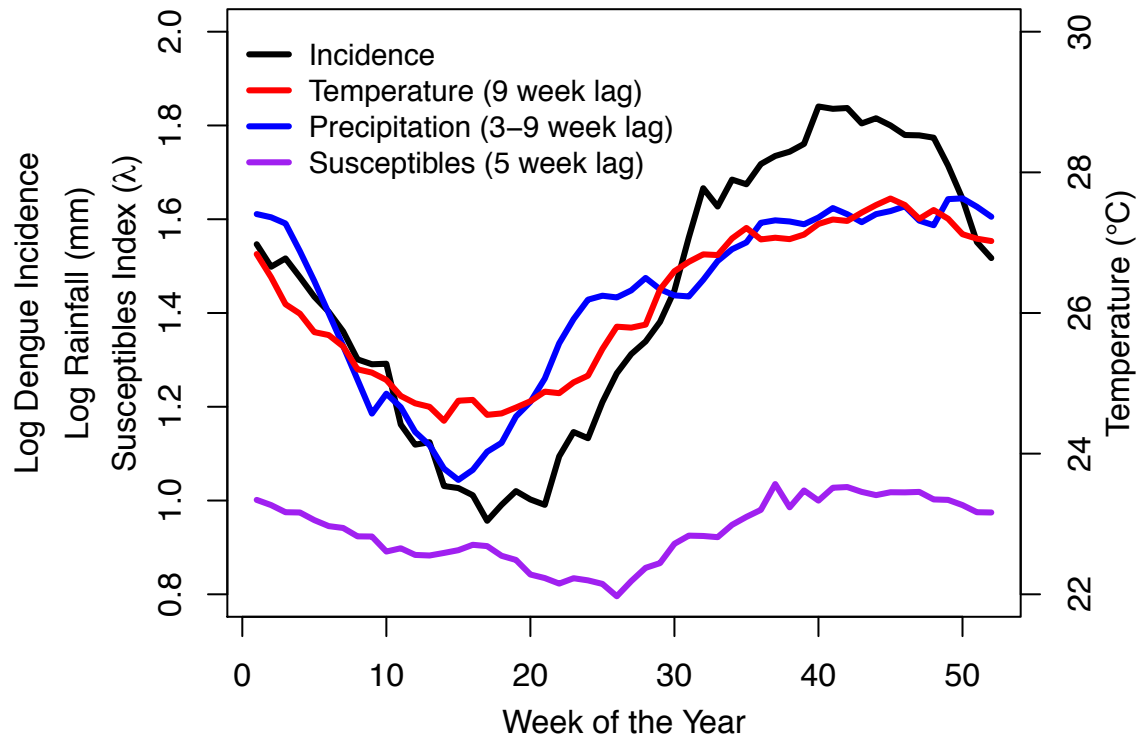
- 697 Watts, D.M., Burke, D.S., Harrison, B.A., Whitmire, R.E. & Nisalak, A. (1987). Effect of  
698 temperature on the vector efficiency of *Aedes aegypti* for dengue 2 virus. *Am. J.*  
699 *Trop. Med. Hyg.*, 36, 143–152.
- 700 Xu, L., Stige, L.C., Chan, K.-S., Zhou, J., Yang, J., Sang, S., *et al.* (2017). Climate variation  
701 drives dengue dynamics. *Proc. Natl. Acad. Sci.*, 114, 113–118.
- 702 Zhao, S., Musa, S.S., Hebert, J.T., Cao, P., Ran, J., Meng, J., *et al.* (2020). Modelling the  
703 effective reproduction number of vector-borne diseases: The yellow fever  
704 outbreak in Luanda, Angola 2015-2016 as an example. *PeerJ*, 2020.
- 705

706 **FIGURES**



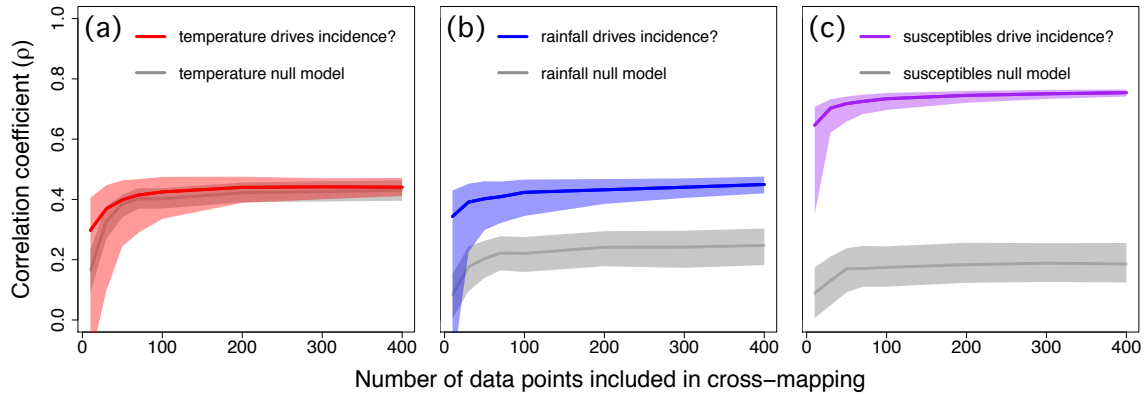
707

708 **Figure 1. Dengue incidence, climate, and susceptibles index data.** Time series  
709 (seasons 1990/1991–2008/2009) of (a) weekly dengue incidence (i.e., total number  
710 of cases per week), (b) weekly average temperature, (c) total weekly rainfall, and  
711 (d) a proxy for susceptible population size (see Supporting Information for details)  
712 in San Juan, Puerto Rico.



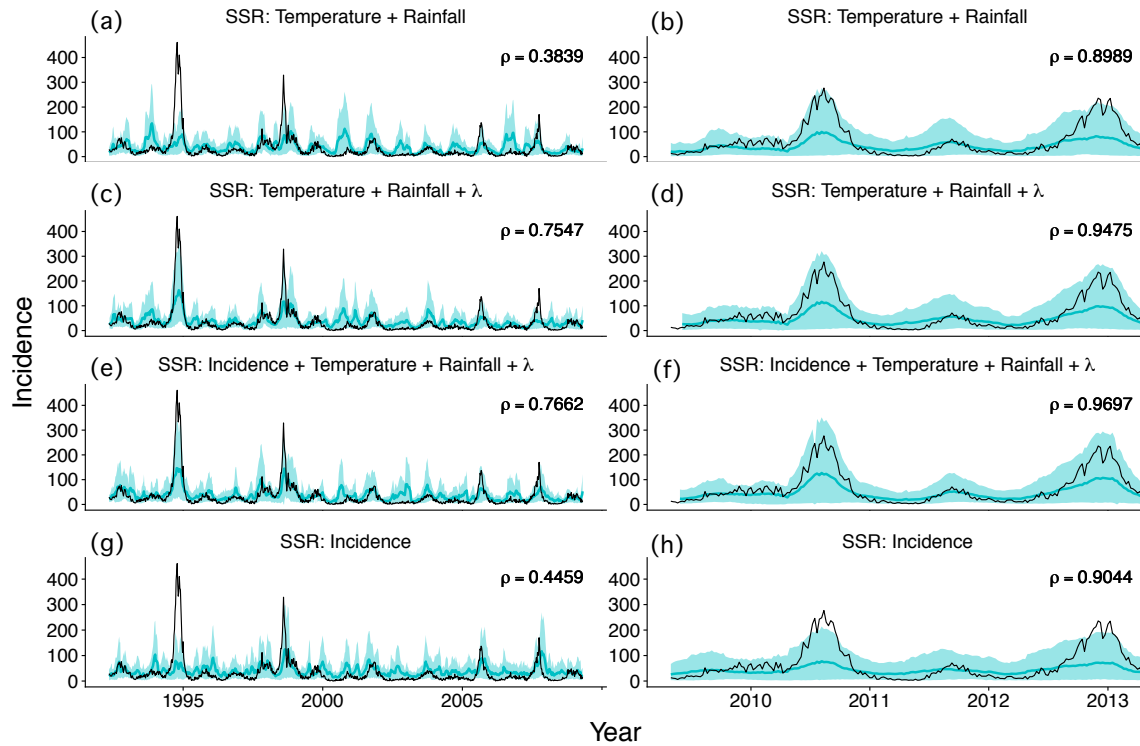
713

714 **Figure 2. Seasonal trends and lags of dengue incidence and its drivers.** The  
715 strong seasonal signal of dengue cases and other variables suggests potential causal  
716 lags between dengue incidence and temperature, rainfall, or the proxy for the  
717 susceptible population size. The lines represent interannual averages for each week  
718 of the year (i.e., calendar week) of dengue incidence (black), temperature shifted 9  
719 weeks forward in time (red), average rainfall over the preceding 3–9 weeks and  
720 shifted 3 weeks forward in time (blue), and susceptibles index shifted 5 weeks  
721 forward in time (purple).



722

723 **Figure 3. Climate and susceptibles index drive dengue incidence.** Cross-  
724 mapping between dengue incidence and temperature (a; red), rainfall (b; blue), or  
725 susceptibles index (c; purple) display significant (Kendall's  $\tau > 0$ ;  $P < 0.01$ )  
726 convergence in cross-mapping skill (i.e.,  $\rho$  increases and reaches an asymptote) as  
727 the length of the time series increases (a signal of putative causality). Red, blue and  
728 purple shaded regions represent the 0.025 and 0.975 quantiles of bootstrapped  
729 time series segments. Grey shaded regions represent the 0.025 and 0.975 quantiles  
730 of the seasonal null distributions obtained from 500 runs of randomized time series  
731 with conserved seasonal trends (Deyle *et al.* 2016a). Solid lines represent medians  
732 of distributions. Rainfall and susceptibles index showed significant forcing above  
733 and beyond seasonal signal (K-S  $P < 0.0001$ ), because cross-mapping of the true  
734 time series (blue and purple) are distinguishable from their respective null models  
735 (grey), whereas temperature forcing was not distinguishable from the null (K-S  $P =$   
736 0.90).



737

738 **Figure 4. Predictive power of climate and susceptibles index ( $\lambda$ ) on in-sample**

739 **(left) and out-of-sample (right) dengue incidence.** Forecasting results of

740 incidence (8 weeks ahead) are shown in turquoise (solid lines represent the mean;

741 shaded regions represent 90% confidence intervals) and observed incidence in

742 black. (a, c, e, g) Time series for seasons 1990/1991–2008/2009 were used to

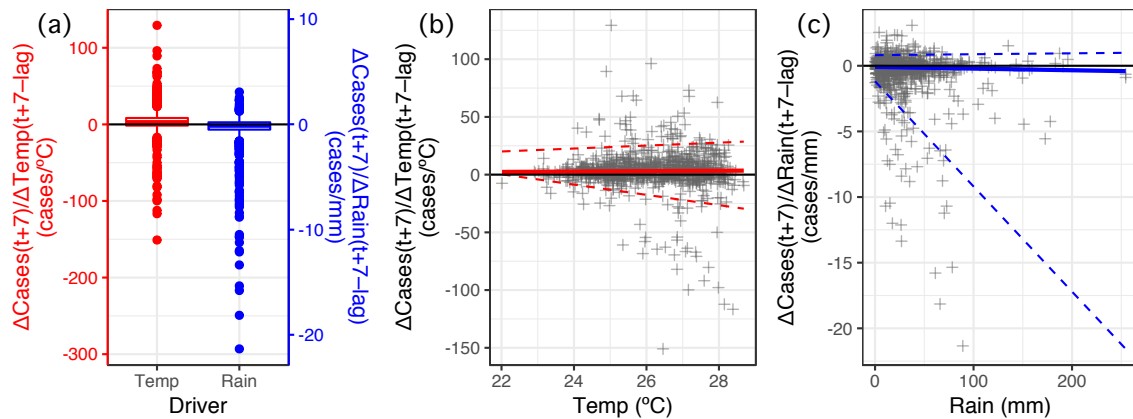
743 construct SSR models for forecasts using leave-one-out cross-validation. (b, d, f, h)

744 Data for seasons 2009/2010–2012/2013 were used to evaluate the SSR models

745 constructed in a, c, e, and g, respectively, for out-of-sample forecasts. All SSR models

746 (a–h) had significant forecasting skill ( $\rho$ ) values (Fisher's z-transformation  $P <$

747 0.001).



748

749 **Figure 5. Temperature and rainfall show mixed effects on dengue incidence.**

750 Scenario exploration quantified the variable effect of changes in drivers on dengue.

751 Boxplots show that the median effects of rainfall (Rain) and temperature (Temp) are

752 small (close to zero), but drivers occasionally have strong impacts (a). To investigate

753 climate driver functional responses, we plotted the rate of change of dengue

754 incidence as a function of temperature (b) and rainfall (c). Red and blue lines

755 represent regression on the median for temperature and rainfall, respectively, in a

756 quantile regression. The dashed red and blue lines represent regression on the 0.05

757 and 0.95 quantiles of temperature and rainfall, respectively. Temperature has an

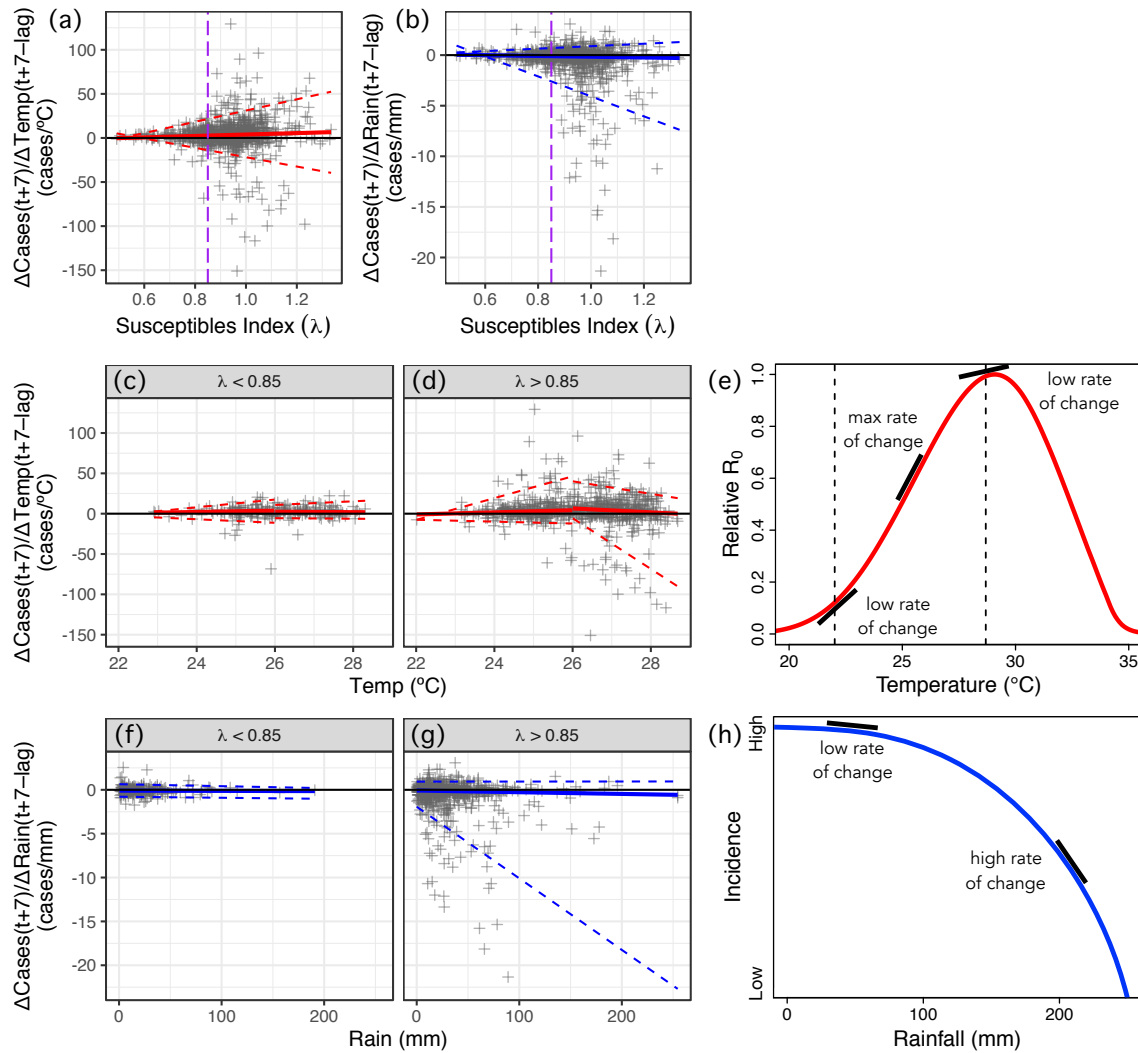
758 overall positive effect on dengue incidence (median regression line of the rate of

759 change is positive), but can also have large negative and positive effects (a, b).

760 Rainfall has an overall negative effect (median regression line of the rate of change

761 is negative), but can also have small positive and large negative effects (a, c).





762

763 **Figure 6. Temperature and rainfall effects on dengue incidence vary**

764 **depending on the susceptible population size ( $\lambda$ ).** The effect of changes in

765 temperature (a) and rainfall (b) against  $\lambda$  shows that driver effects are split around

766 the threshold  $\lambda \approx 0.85$  (purple dashed line). The red and blue lines represent the

767 median regression of temperature and rainfall effects, respectively, in a quantile

768 regression (a-d, f, g). The dashed red and blue lines represent the 0.05 and 0.95

769 quantile regressions of temperature and rainfall effects, respectively (a-d, f, g).

770 Neither driver has an effect on dengue incidence when susceptible availability is low

771 ( $\lambda < 0.85$ ; c, f). However, when  $\lambda > 0.85$  climate effects are observed: temperature  
772 has mostly a positive effect (d), possibly sigmoidal in that temperature range (e),  
773 and rainfall has a negative effect (g), and conceptually a concave down functional  
774 response (h; black lines represent tangents, where the slope of the tangent is the  
775 rate of change). The effect of temperature on relative  $R_0$  of dengue assuming  
776 transmission via *Aedes aegypti* mosquitoes is unimodal (Mordecai *et al.* 2017) over a  
777 large temperature range (e; dashed lines indicate the minimum and maximum  
778 temperature values in the data of our study, black lines represent tangents, where  
779 the slope of the tangent is the rate of change of relative  $R_0$  of dengue as a function of  
780 temperature). Assuming that relative  $R_0$  is proportional to dengue incidence, our  
781 results suggest that the rate of change of dengue incidence is increasing until  
782 reaching a maximum and then decreasing (d; red median regression lines).  
783 However, even when driver effects are split at the evident threshold of  $\lambda = 0.85$  (c,  
784 d, f, g), there are still many occurrences when the susceptible population size is  
785 sufficient large ( $\lambda > 0.85$ ) but temperature and rainfall have no effect. In certain  
786 cases, temperature has even a negative effect on dengue (d).